Plasma Sources Sci. Technol. **17** (2008) 045018 (6pp) doi:10.1088/0963-0252/17/4/045018

Influence of gas heating on high pressure dc microdischarge I–V characteristics

Sergey G Belostotskiy, Vincent M Donnelly and Demetre J Economou

Plasma Processing Laboratory, Department of Chemical and Biomolecular Engineering, University of Houston, Houston, TX 77204-4004, USA

E-mail: vmdonnelly@uh.edu and economou@uh.edu

Received 7 January 2008, in final form 4 July2008
Published 1 September 2008
Online at stacks.iop.org/PSST/17/045018

Abstract

Experimental I–V characteristics of dc microdischarges in helium at different operating pressures ($p = 300$–800 Torr) reveal that the classical scaling law of the cathode layer (sheath) does not apply. It is shown that a modified semi-analytical model of the cathode layer that accounts for neutral gas heating is able to reproduce the trends of the experimental I–V characteristics. The model can also be used to quantify the influence of gas heating on microdischarge characteristics and to estimate conditions for stable operation of microdischarges.

1. Introduction

High pressure (100s of Torr) non-equilibrium microdischarges have been the subject of intense investigations over the past decade [1–15]. A combination of unique characteristics (dimension of 100s of micrometres, atmospheric pressure operation, power density of 10–100 kW cm^{-3}) favours many applications of such microdischarges, including excimer radiation sources, sensors, plasma display panel cells, ozone sources, microreactors for surface treatment or biomedical applications, etc [3–7]. Despite advances in fundamental understanding, many questions still remain regarding the physics of microdischarges. For instance, to what extent are 'scaling laws' developed for large-scale gas discharges ($p \sim 0.1$–10 Torr, $L \sim 1$–100 cm) applicable to their micro-scale counterparts?

von Engel and Steenbeck developed a (now classical) theory of the cathode layer of a dc discharge [16–18] (henceforth in this paper to be called the 'classical theory'). For a specific gas and electrode material, the voltage drop (V_c) across the cathode layer (sheath) was found to be a function of the so-called reduced current density, i.e. the ratio between the discharge current density (j) and the square of gas pressure (p^2) or $V_c = f(j/p^2)$. A typical current–voltage (I–V) characteristic based on this theory is presented in figure 1. The right-hand branch of the curve corresponds to an *abnormal* discharge; the minimum corresponds to a *normal* discharge and the left-hand branch corresponds to an unstable *subnormal* discharge that is usually not observed in experiments.

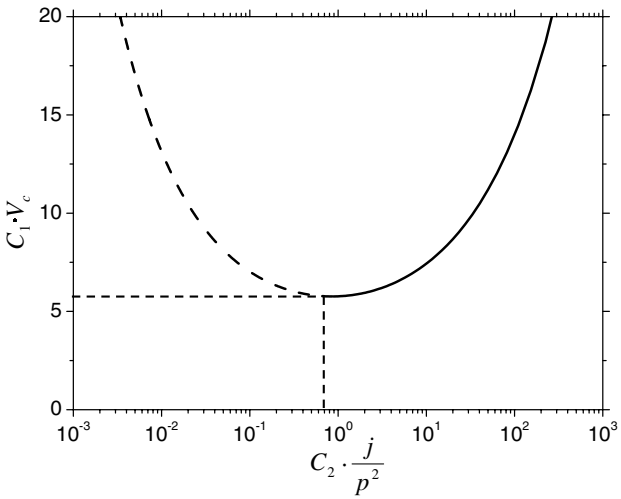

Figure 1. I–V characteristic of the cathode layer of a dc discharge [16]; constants C_1 and C_2 depend on gas and electrode material.

This classical scaling law is known to work well for conventional large-scale dc discharges. In order to check the validity of this relation in microscale discharges, the I–V characteristics of a helium microdischarge were recorded for different pressures.

2. Experiment

A slot-type dc helium microdischarge (figure 2(*a*)) was used for experimental work. The spacing between the rectangular

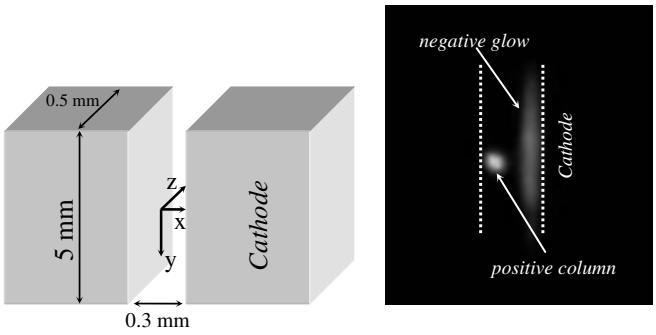

Figure 2. (*a*) Schematic diagram of the slot-type microdischarge used for experimental work. (*b*) Image of a helium microdischarge ($p = 600$ Torr, $I = 10$ mA). The dashed lines show the approximate location of the electrodes.

(5 mm × 0.5 mm exposed area) molybdenum electrodes was $L = 300\,\mu$m and the operating pressure was varied in the range $p = 300$–800 Torr. Such operating conditions ($pL \sim 10$ Torr cm) correspond to a discharge with a short positive column (figure 2(*b*)).

The electric field in the positive column is determined by the electron density balance, i.e. electron production must equal electron loss. As shown in [14], under the present experimental conditions, three-body recombination is the main channel of electron loss,

$$\mathrm{e} + \mathrm{e} + \mathrm{He}_2^+ \longrightarrow \mathrm{He}_2^{**} + \mathrm{e},$$

Using typical values of electron temperature $T_\mathrm{e} \sim 2$ eV and electron density $n_\mathrm{e} \sim 10^{13}\,\mathrm{cm}^{-3}$, one obtains an electron loss frequency of $\sim 10^5\,\mathrm{s}^{-1}$. The electric field necessary to produce an ionization frequency of $10^5\,\mathrm{s}^{-1}$ is $E \sim 1\,\mathrm{kV\,cm}^{-1}$. For a positive column length of $\sim 100\,\mu$m, this results in a voltage drop of ~ 10 V. Since a typical voltage drop across the microdischarge is ~ 200 V, one concludes that the microdischarge voltage is roughly the same as the cathode layer (sheath) voltage (this conclusion is corroborated by a simulation result shown in figure 3(*a*) of [14]). It should also be mentioned that the spacing between the electrodes L is several times larger than the cathode layer thickness d_c ($L > d_\mathrm{c}$), so that the classical glow discharge structure is obtained [19].

The voltage across the microdischarge was measured with a high voltage probe (Tektronix P5100) connected to an oscilloscope (Tektronix 2430). The discharge current was measured as the voltage across a 100 Ω resistor again using an oscilloscope. The oscilloscope was connected to a personal computer via GPIB and data acquisition was controlled by a LabVIEW program.

The experimental I–V characteristics (figure 4) do not follow the classical theory of von Engel and Steenbeck [16–19]. Specifically, the voltage drop across the cathode layer is not solely a function of reduced current density, but it also depends on pressure.

Previous investigations [13–15] have shown that ohmic heating can result in a considerable rise in the neutral gas temperature (T_g) in a microdischarge (T_g may reach ~ 1000 K). In the presence of gas heating, the gas number density N is reduced for an isobaric system (it should be noted here that discharge scaling parameters depend upon gas number density N rather than pressure). Moreover, T_g affects ion mobility and hence ion drift velocity. Thus, gas heating affects the discharge electric field and the current density, and in turn the heat generation term. Therefore, the equations for charged particle transport must be coupled with the heat transfer equation.

The question still remains as to whether or not neutral gas heating is the main reason for the disagreement of the classical theory with the experimental data in atmospheric pressure microdischarges. To answer this question, the classical theory of the cathode layer was modified to include neutral gas heating effects. The goal was to develop a semi-analytical model, the solution of which can provide more insight into the physics of the problem, as compared with a purely numerical solution.

3. Mathematical model

As shown in [14], He^+ is the dominant ion in the cathode layer for this type of microplasma. Thus, only one type of ion was considered in the model.

The system of one-dimensional equations for a steady-state cathode layer is

$$\begin{cases} \dfrac{\partial(n_\mathrm{e} \cdot v_\mathrm{e})}{\partial x} = \alpha \cdot n_\mathrm{e} \cdot v_\mathrm{e} - \beta_\mathrm{r} \cdot n_\mathrm{e} \cdot n_\mathrm{i}, \\ \dfrac{\partial(n_\mathrm{i} \cdot v_\mathrm{i})}{\partial x} = \alpha \cdot n_\mathrm{e} \cdot v_\mathrm{e} - \beta_r \cdot n_\mathrm{e} \cdot n_\mathrm{i}, \\ \dfrac{\partial E}{\partial x} = \dfrac{e}{\varepsilon_0} \cdot (n_\mathrm{i} - n_\mathrm{e}), \\ k \cdot \dfrac{\partial^2 T}{\partial x^2} + j \cdot E = 0. \end{cases} \tag{1}$$

Here n_e and n_i are electron and ion density, respectively, v_e and v_i are electron and ion drift velocity, respectively, α is the ionization (1st Townsend) coefficient, β_r is the recombination coefficient, ε_0 is the permittivity of free space, e is the unit charge, k the is thermal conductivity of He and j is the total current. The boundary condition at the cathode ($x = 0$) is

$$\gamma \cdot n_\mathrm{i}(0) \cdot v_\mathrm{i}(0) = -n_\mathrm{e}(0) \cdot v_\mathrm{e}(0), \tag{2}$$

where γ is the secondary electron emission coefficient.

To simplify the model, the following 'standard' approximations were made [16–19].

(1) Electron–ion recombination is negligible because of the low electron density in the cathode layer.
(2) The electric field (E) decreases linearly with distance, i.e.

$$E(x) = -E_\mathrm{c} \cdot \left(1 - \frac{x}{d_\mathrm{c}}\right), \tag{3}$$

where E_c is the electric field at the cathode.
(3) The ionization coefficient can be approximated by

$$\alpha(E, N) = A \cdot N \cdot \exp\left\{-\frac{B \cdot N}{|E|}\right\}, \tag{4}$$

where A and B are constants for a specific gas. In the present case, $A = 3.11\,\mathrm{cm}^{-1}\,\mathrm{Torr}^{-1}$ and

$B = 80.85\,\mathrm{V\,cm^{-1}\,Torr^{-1}}$ were extracted by fitting the experimental data by Chanin and Rork [20] at high ($>20\,\mathrm{V\,cm^{-1}\,Torr^{-1}}$) E/p.

(4) The cathode layer thickness d_c is determined by the relation

$$j_e(d_c) \approx j, \tag{5}$$

where j_e is the electron current density.

(5) At low reduced electric fields (typically for E/N less than ~50 Td) the ion drift velocity is a linear function of E/N [17–19]. This implies that the ion mobility is independent of E/N and

$$\mu_i \propto \frac{1}{N \cdot \sqrt{T}} \qquad \text{or} \qquad \mu_i \cdot p \propto \sqrt{T}. \tag{6}$$

It follows that, for constant gas temperature (and assuming that the ion temperature is equal to the gas temperature), $\mu_i \cdot p = \text{const}$. However, at high E/N (typically for E/N greater than ~200 Td) the ion drift velocity depends on $\sqrt{E/N}$. This means that the ion mobility decreases as $(1/\sqrt{E})$, or

$$\mu_i \cdot p \propto \sqrt{\frac{p}{E}} \cdot \sqrt{T}. \tag{7}$$

The classical theory [17–19] employs equation (6) for ion mobility, where $\mu_i p = \text{const}$, since the gas temperature is assumed constant (no gas heating). However, since the reduced electric field in the cathode region typically exceeds ~100 Td, it is expected that equation (7) is more appropriate and it was used for further analysis. It should be emphasized that, assuming a constant temperature, the classical scaling law, $V_c = f(j/p^2)$, is independent of what expression is used for the ion mobility (equation (6) versus equation (7)). The expression used for ion mobility in this work is

$$\mu_i = \sqrt{\frac{C}{E \cdot p}} \cdot \sqrt{\frac{T}{T_0}}, \tag{8}$$

where C is a constant determined by fitting experimental data by Helm [21] in the E/N range of interest.

In addition to the above approximations, the following simplifications were made regarding the thermal properties of the system.

(6) The gas thermal conductivity is independent of temperature.

(7) In order to obtain a semi-analytical solution, a spatially averaged gas temperature $\langle T \rangle$ was used for the cathode layer, such that the gas number density is $N = p/k_b \cdot \langle T \rangle$, where k_b is the Boltzmann constant.

Taking into account the assumptions stated above, the fourth equation of system (1) can be reduced to a steady-state heat transfer problem with a source term given by

$$W = \begin{cases} |j| \cdot E_c \cdot \left(1 - \dfrac{x}{d_c}\right), & \text{for } 0 < x < d_c, \\ 0, & \text{for } d_c < x < L. \end{cases} \tag{9}$$

The solution of this equation with constant temperature T_0 at the electrode gives the following expression for the average temperature in the cathode layer:

$$\frac{\langle T \rangle}{T_0} - 1 = \frac{1}{2} \frac{|j| \cdot E_c}{k \cdot T_0} \cdot \Lambda^2, \tag{10}$$

where

$$\Lambda^2 = \frac{1}{6} \cdot d_c^2 \cdot \left(\frac{3}{2} - \frac{d_c}{L}\right) \qquad \text{and}$$

$$\langle T \rangle = \frac{\int_0^{d_c} T(x)\,\mathrm{d}x}{d_c}.$$

It should be pointed out that, at or near atmospheric pressure, ions do not gain much energy in the sheath, due to the high collisionality. For example, for a pressure of 500 Torr, the ion mean free path λ is ~100 nm. Thus, near the cathode, ions gain energy equal to $(e \cdot E_c \cdot \lambda) \sim 1$ eV. (E_c is the cathode field.) When this energy is multiplied by the ion current to the cathode and the cathode area, the power deposited by ion bombardment on the cathode is ~0.05 W, much less than the total power ($I \cdot V_c \sim 4$ W) dissipated in the cathode layer.

The value of T_0 was chosen to be 350 K. This assumes that the cathode temperature is maintained constant at this value. No control of the cathode temperature was exercised in this study. However, the microdischarge was part of a block that, by virtue of its large heat capacity, moderated temperature excursions of the cathode. Thermocouple measurements of the cathode temperature in another study under similar microdischarge geometry and operating conditions showed that the cathode temperature did not exceed 420 K. The value chosen (350 K) represents an average temperature.

Solving the first two equations of system (1) and using the boundary condition equation (2), one obtains the following expressions for the electron and ion current:

$$j_e(x) = -\gamma \cdot e \cdot v_i(0) \cdot n_i(0) \cdot \exp\left\{\int_0^x \alpha(E(x), N)\,\mathrm{d}x\right\}, \tag{11}$$

$$j_i(x) = -e \cdot v_i(0) \cdot n_i(0) \cdot \left[1 + \gamma - \gamma \cdot \exp\left\{\int_0^x \alpha(E(x), N)\,\mathrm{d}x\right\}\right]. \tag{12}$$

The total current is the sum of the electron and ion currents,

$$j = -e \cdot v_i(0) \cdot n_i(0) \cdot (1 + \gamma), \tag{13}$$

where γ is the secondary electron emission coefficient. Solving the third equation of system (1) and using the electric field given by equation (3):

$$\frac{E_c}{d_c} = \frac{e}{\varepsilon_0} \cdot (n_i(x) - n_e(x)) = \frac{e}{\varepsilon_0} n_i(0). \tag{14}$$

Solving equation (14) for $n_i(0)$, plugging it into equation (13) and taking into account equation (8) results in

$$j = -\sqrt{\frac{C}{p}} \cdot \varepsilon_0 \cdot \frac{E_c^{3/2}}{d_c} \cdot (1 + \gamma) \cdot \sqrt{\frac{\langle T \rangle}{T_0}}. \tag{15}$$

Using equation (5) one obtains

$$\int_0^{d_c} \alpha(|E(x)|, N)\,\mathrm{d}x = \ln\left(\frac{1+\gamma}{\gamma}\right), \tag{16}$$

which is essentially an equation for the electric field E_c, taking into account equation (4). Excluding the explicit dependence on temperature, equations (15) and (16) look identical to the ones in [17–19]. However, in the presence of gas heating, these equations are coupled with equation (10).

Substituting the current density given by equation (15) into equation (10),

$$\frac{\langle T\rangle}{T_0} - 1 = \frac{\Lambda^2}{k\cdot T_0}\cdot\frac{1}{2}\cdot\frac{E_c^{5/2}}{d_c}\cdot\varepsilon_0\cdot(1+\gamma)\cdot\sqrt{\frac{C}{p}}\cdot\sqrt{\frac{\langle T\rangle}{T_0}}. \tag{17}$$

Solving equation (17) for $\langle T\rangle/T_0$ and substituting $E_c = 2\cdot V_c/d_c$,

$$\frac{\langle T\rangle}{T_0} = \frac{1}{4}\cdot\left(\beta\cdot\frac{V_c^{5/2}}{d_c^{7/2}} + \sqrt{\beta^2\cdot\frac{V_c^5}{d_c^7}+4}\right)^2 = \theta(V_c, d_c, p), \tag{18}$$

where

$$\beta = 2\cdot\varepsilon_0\cdot\frac{\Lambda^2}{k\cdot T_0}\cdot(1+\gamma)\cdot\sqrt{\frac{2\cdot C}{p}}.$$

Plugging this expression into equation (16) yields the final equation that implicitly determines the dependence of the cathode voltage drop on the cathode layer thickness $V_c(d_c)$:

$$A\cdot B\cdot\left(\frac{p\cdot d_c}{k_b\cdot T_0}\right)^2\cdot(\theta(V_c, d_c, p))^{-2}\cdot\frac{1}{2\cdot V_c} \cdot\Phi\left(\frac{2\cdot V_c\cdot k_b\cdot T_0}{B\cdot p\cdot d_c}\cdot\theta(V_c, d_c, p)\right) = \ln\left(\frac{1+\gamma}{\gamma}\right), \tag{19}$$

where

$$\Phi(z) = \int_0^z \exp\left(-\frac{1}{t}\right)\mathrm{d}t.$$

Substituting $V_c(d_c)$ into the equation for current density, equation (15), provides an expression for the current density as a function of voltage:

$$j = -\sqrt{\frac{2\cdot C}{p}}\cdot 2\cdot\varepsilon_0\cdot\frac{V_c^{3/2}}{d_c^{5/2}}\cdot(1+\gamma)\cdot\sqrt{\theta(V_c, d_c, p)}, \tag{20}$$

At this point one can observe that since $\theta \neq f(p\cdot d_c)$, the solution of equation (19) will not be a function of $p\cdot d_c$, i.e. $V_c \neq f_1(p\cdot d_c)$. It is also evident from equation (20) that the reduced current density is not a function of $p\cdot d_c$, i.e. $j/p^2 \neq f_2(p\cdot d_c)$. Thus $V_c \neq f(j/p^2)$, i.e. the classical scaling is not valid.

4. Results and discussion

At low pressure (e.g. 1 Torr), for which the classical theory is known to work, the solution of equation (19) almost coincides with the solution of von Engel and Steenbeck (shown as the dashed line in figure 3). In practice, divergence from the classical solution can occur even for low pressures, provided the power deposition is high enough to cause considerable gas heating.

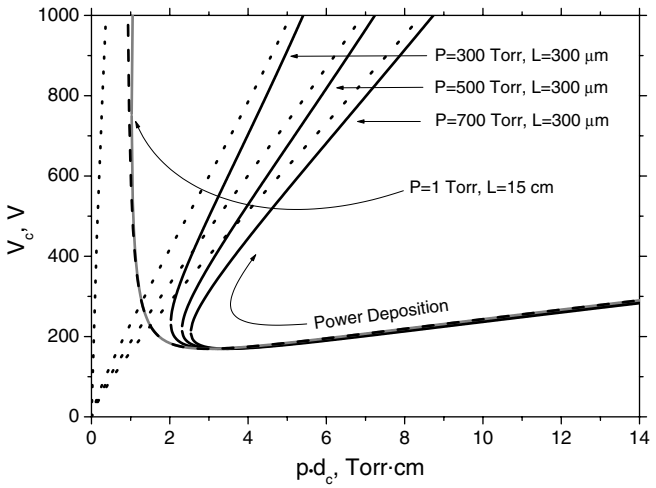

Figure 3. Cathode voltage drop versus $p\cdot d_c$ for different pressures and interelectrode gaps. The solid lines are solutions of equation (19), the dotted lines are thermal asymptotes and the dashed line is the solution of von Engel and Steenbeck. Note that $p\cdot L$ is the same for $p = 1$ Torr and $p = 500$ Torr. Power deposition increases in the direction of the arrow.

When gas heating is severe, one can obtain an asymptotic solution to equation (19). At this extreme, equation (18) reduces to

$$\frac{\langle T\rangle}{T_0} \approx \beta^2\cdot\frac{V_c^5}{d_c^7} \gg 1. \tag{21}$$

Taking into account that $\Phi(z) \to z$ for $z \gg 1$, an explicit expression for V_c may be obtained for this 'thermal asymptote,'

$$V_c = \left[\frac{A}{k_b\cdot T_0\cdot\ln\left(\frac{1+\gamma}{\gamma}\right)}\cdot\frac{p\cdot d_c^8}{\beta^2}\right]^{1/5}. \tag{22}$$

Solutions of equation (19), as well as the corresponding thermal asymptotes, for different gas pressures and interelectrode gaps are also presented in figure 3. The direction of the 'power deposition' arrow corresponds to increasing power deposition in the discharge. At low power, gas heating is negligible and all curves collapse on top of one another (classical theory is applicable). At high power, gas heating becomes important and the curves separate from one another.

As seen in figure 3, at some specific value of $p\cdot d_c$ (depending on pressure) the solution of equation (19) has a turning point. The branch that lies above this point quickly tends to the thermal asymptote (the dotted lines). In practice, this will happen at high enough power deposition, causing the glow discharge to transition into an arc. Although accurate prediction of the glow-to-arc transition is beyond the capabilities of the simple model presented here, the turning point in figure 3 can provide a rough criterion for glow discharge stability. (The gas temperatures at the turning points

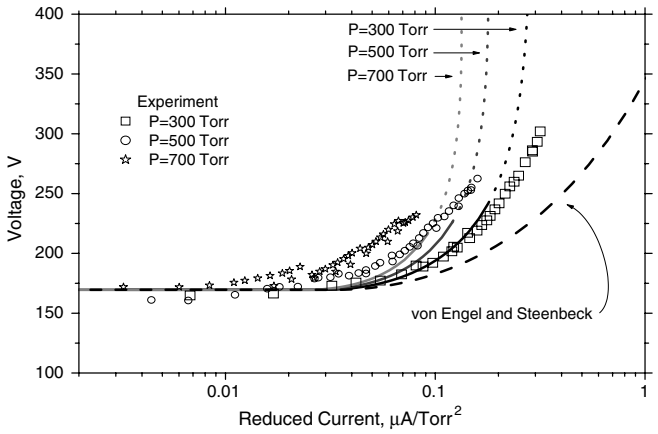

Figure 4. I–V characteristics of helium microdischarges. Points are experimental data. The solid and the dotted lines are theoretical curves corresponding to stable and unstable operation, respectively. The dashed line is the result obtained using the classical theory.

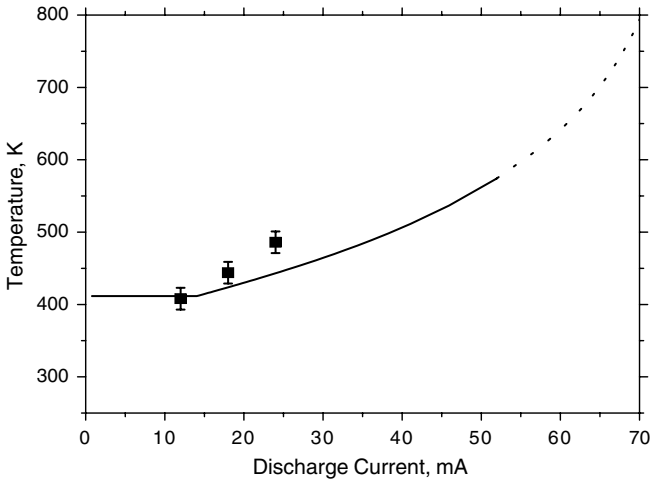

Figure 5. Gas temperature averaged across the cathode layer of a He microdischarge at $p = 760$ Torr. The data points are results of Wang *et al* [13]. The solid and the dotted lines are predictions of the model, corresponding to stable and unstable regions, respectively.

were calculated to be 498 K, 538 K and 564 K, for pressures of 300 Torr, 500 Torr and 700 Torr, respectively.)

The turning point can be found from the following system of equations:

$$\begin{cases} f(V_c, d_c, p) = A \cdot B \cdot \left(\dfrac{p \cdot d_c}{k_b \cdot T_0}\right)^2 \cdot (\theta(V_c, d_c, p))^{-2} \\ \quad \cdot \dfrac{1}{2 \cdot V_c} \cdot \Phi\left(\dfrac{2 \cdot V_c \cdot k_b \cdot T_0}{B \cdot p \cdot d_c} \cdot \theta(V_c, d_c, p)\right) \\ \quad = \ln\left(\dfrac{1+\gamma}{\gamma}\right), \\ \dfrac{\partial f(V_c, d_c, p)}{\partial V_c} = 0. \end{cases} \tag{23}$$

It is known [17–19] that the branch of the I–V curve with $j < j_n$ (j_n is the normal current density) is not realized in experiments. Instead, when the discharge current is less than $I_n = j_n \cdot S_c$ (S_c is the cathode surface area), further decrease in current is accompanied by a decrease of the size of the cathode current spot, so that the current density remains constant, equal to the normal current density (this is called normal discharge). In a normal discharge, the cathode voltage drop is independent of current. It turns out that the current density (and voltage) remains constant, even in the presence of gas heating [22]. The transition to the normal discharge occurs at the minimum voltage V_n of the theoretical I–V characteristic (the minimum of the curve in figure 1).

I–V curves obtained by solving equations (19) and (20) are compared with experimental data in figure 4. To compare with the measured quantity (current) directly, the theoretical current density (j_n) was converted to current (I) as follows: for $I \geqslant j_n \cdot S_c$ ($S_c = 0.025\,\mathrm{cm}^2$ is the known cathode surface area) the calculated voltage was plotted versus $(j \cdot S_c)/p^2$. For $I < j_n \cdot S_c$, the voltage was set equal to V_n (normal voltage drop). The only 'adjustable' parameter in the model was the secondary electron emission coefficient γ. The value of $\gamma = 0.13$ was chosen so that the resulting theoretical normal cathode potential V_n fits the experimental data at low current. The model captures the trends in the experimental data fairly well. For a given pressure (300, 500 and 700 Torr), the end of the solid line corresponds to the turning point of figure 3. The dotted line corresponds to the unstable branch (the branch above the turning point in figure 3). For this unstable branch, the voltage drop (and therefore the power deposition) goes up rapidly (dotted lines in figure 4 are almost vertical). This would cause severe gas heating and breed conditions for a glow-to-arc transition.

The present model cannot capture the (negative slope) I–V characteristic of the arc without invoking additional physical mechanisms. The model simply provides a rough estimate of parameter values conducive to transition to arc. It should also be mentioned that, for each pressure, the rightmost experimental data point in figure 4 corresponds approximately to the highest current at which the microdischarge could be operated, before transitioning into an arc. Thus, the criterion for microdischarge stability proposed here seems to work reasonably well.

In order to justify the validity of the present model, gas temperatures were estimated for the conditions of the experiment described in [13]. The only difference between the system used in this experiment and the one in [13] was the spacing between the electrodes. Since the temperature predicted by the model is the average temperature across the cathode layer, the spatially resolved measurements presented in [13] were also averaged over the cathode, the size of which was determined from the model, for each value of current. The thickness of the cathode layer ($p = 760$ Torr) varied from $d_c = 39\,\mu$m at $I = 24$ mA to $d_c = 46\,\mu$m at $I = 12$ mA. A comparison of experimental data [13] and the results of the model is presented in figure 5. Theoretical predictions for the gas temperature agree well with the measurements. Thus the model is able to provide good estimates and trends for gas temperatures in microdischarges.

Since the secondary electron emission coefficient γ was the only 'adjustable' parameter in the model, the sensitivity of the I–V characteristics on γ should be ascertained. As seen in figure 6, the normal cathode voltage drop is very sensitive to the value of γ. However, the shape of the curve and the

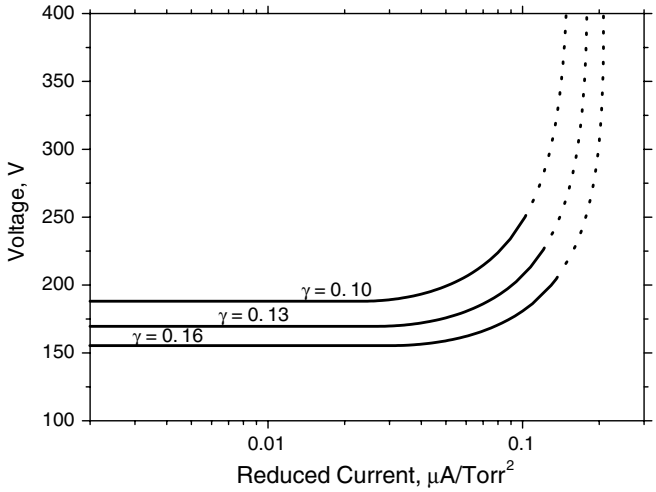

Figure 6. Theoretical I–V characteristics of a He microdischarge at $p = 500$ Torr for different γ. The solid and the dotted lines are predictions of the model, corresponding to stable and unstable regions, respectively.

value of the normal current density are relatively insensitive to variations in γ.

5. Conclusions

Measured I–V characteristics of high pressure dc microdischarges in helium showed that the classical scaling law, namely that the cathode layer voltage is a function of the reduced current density, $V_c = f(j/p^2)$, is not valid. The classical theory of the cathode layer was modified to account for neutral gas heating. The resulting semi-analytical model reproduced the trends of the experimental I–V characteristics in a semi-quantitative manner. Furthermore, the model was used to obtain a rough criterion of the glow-to-arc transition.

References

[1] Becker K H, Schoenbach K H and Eden J G 2006 *J. Phys. D: Appl. Phys.* **39** R55
[2] Kushner M 2005 *J. Phys. D: Appl. Phys.* **38** 1633
[3] Kogelschatz U 2004 *Plasma Phys. Control. Fusion* **46** B63
[4] Boeuf J P 2003 *J. Phys. D: Appl. Phys.* **36** R53
[5] Tachibana K, Kawai S, Asai H, Kikuchi N and Sakamoto S 2005 *J. Phys. D: Appl. Phys.* **38** 1739
[6] Sarra-Bournet C, Turgeon S, Mantovani D and Laroche G 2006 *J. Phys. D: Appl. Phys.* **39** 3461
[7] Sladek R E J and Stoffels E 2005 *J. Phys. D: Appl. Phys.* **38** 1716
[8] Sakiyama Y and Graves D B 2006 *J. Phys. D: Appl. Phys.* **39** 3451
[9] Wilson C G, Gianchandani Y B, Arslanbekov R R, Kolobov V and Went A E 2003 *J. Appl. Phys.* **94** 2845
[10] Ivanov V V, Klopovskii K S, Mankelevich Yu A, Rakhimov A T, Rakhimova T V, Rulev G B and Saenko V B 1996 *Laser Phys.* **6** 654
[11] Arkhipenko V I, Kirillov A A, Simonchik L V and Zgirouski S M 2005 *Plasma Sources Sci. Technol.* **14** 757
[12] Yalin A P, Laux C O, Kruger C H and Zare R N 2002 *Plasma Sources Sci. Technol.* **11** 248
[13] Wang Q, Koleva I, Donnelly V M and Economou D J 2005 *J. Phys. D: Appl. Phys.* **38** 1690
[14] Wang Q, Economou D J and Donnelly V M 2006 *J. Appl. Phys.* **100** 023301
[15] Belostotskiy S G, Wang Q, Donnelly V M, Economou D J and Sadeghi N 2006 *Appl. Phys. Lett.* **89** 251503
[16] von Engel A and Steenbeck M 1934 *Elektrische Gasentladungen: Ihre Physik and Technik* vol II (Berlin: Springer)
[17] von Engel A 1983 *Electric Plasmas: Their Nature and Uses* (New York: Taylor and Francis)
[18] von Engel A 1994 *Ionized Gases* (Woodbury, NY: AIP)
[19] Raizer Yu P 1991 *Gas Discharge Physics* (Berlin: Springer)
[20] Chanin L M and Rork G D 1964 *Phys. Rev.* **133** 1005
[21] Helm H 1977 *J. Phys. B: At. Mol. Phys.* **10** 3683
[22] Raizer Yu P and Mikhail Shneider N 1999 *IEEE Trans. Plasma Sci.* **27** 701